CrossMark

Structural, optical and electrical properties of Ni doped ZnO nanostructures synthesized by solution combustion method

Harpreetpal Singh[1] · Vijay Kumar[1] · H. C. Jeon[2] · T. W. Kang[2] · Sunil Kumar[2]

Abstract In this work, pure and Ni-doped ZnO nanostructures (NSs) with different concentrations of Ni (2, 4, 6%) were successfully prepared via solution combustion method. The TEM photograph shows the formation of flake-like structures with the decrease in size of NSs as the dopant concentration is increased. XRD investigation shows the hexagonal wurtzite structure of doped and undoped ZnO nanostructures with a NiO peak (200) as secondary phase for 4 and 6% dopant concentration level. Broadening of spectra of ZnO around 480 cm^{-1} in FTIR spectra is observed with the increase of dopant concentration. UV–Visible spectra show the increase in absorbance when the dopant level (Ni^{2+}) is increase from 2 to 4% in ZnO and decrease in absorbance with further increase in dopant level to 6%. An increase in energy band gap is observed in Ni (6%)-doped ZnO due to due to the sp–d interactions taking place between the band electrons and the localised d electrons of Ni^{2+} ions (Burstein-Moss effect). I–V characteristics reveal the increase in current with the increase in dopant level from 2 to 4% and decrease in current when the dopant level is further increased to 6% which is in agreement with the Burstein-Moss effect.

✉ Sunil Kumar
sunilkumar32@gmail.com

1 I.K. Gujral Punjab Technical University, Kapurthala 144603, India

2 Quantum Functional Semiconductor Research Center, Nano Information Technology Academy, Dongguk University, Seoul 100715, South Korea

1 Introduction

Progress in group II–VI semiconductor nano structures has lead advancement to a wide variety of material system [1–4]. Due to high transmittance in the visible region of electromagnetic spectrum, low resistivity, high energy band gap (3.37 eV), large exciton binding energy (60 meV), easy fabrication and non-toxicity; zinc oxide (ZnO) find its potential applications in technological devices such as Field emission displays, solar cells, piezoelectric devices, gas sensors, LEDs, UV light emitters, phototherapy agents etc [5–12 and references therein]. It is well known that the optical, electrical, and magnetic properties of the material could be altered by adding impurities in to a wide band gap semiconductor, thus doping a certain element into ZnO has become an important route for to optimizing its optical, electrical, and magnetic performance, which are crucial for their practical applications [13, 14]. As ZnO bond is ionic as well as covalent, doping in ZnO is much easier compared to other covalent bonded wide band gap semiconductors. Furthermore, Ni^{2+} (0.69 Å) have the same valence compared to Zn^{2+} and its radius is close to Zn^{2+} (0.74 Å), so it is very easy for Ni^{2+} sub-lattice to replace Zn^{2+} in ZnO lattice. Studies on Ni doped ZnO nanostructures prepared by sputtering, spray pyrolysis, pulsed laser deposition, vapor phase, sol–gel, bioassisted process, co-precipitation process etc. have been reported [15–20] and several results showed that the various properties of ZnO were changed after inserting Ni into ZnO matrix. However, the structural, optical properties of Ni–ZnO nanostructures synthesized using solution combustion technique have rarely been described. Solution combustion technique is an easy and simple root to synthesise semiconductor oxide materials. This technique is also known as flame synthesis .In this study, we investigated the structural, optical and electrical properties of Ni doped ZnO

nanostructures with various Ni doping amounts and compared them with undoped ZnO nanostructures.

2 Experimental

Pure and Ni doped ZnO nanoparticles were synthesised by using simple solution combustion technique. To synthesis pure ZnO nanoparticles appropriate proportion of zinc nitrate and urea were mixed and completely dissolved in deionised water. After heating the solution on hot plate it gets converted into gel form which further swelled into foam and after strong combustion ZnO nano powder was produced. The above procedure was repeated by adding appropriate amount of nickel nitrate into the mixture of zinc nitrate and urea to produce 2, 4, 6% Ni doped ZnO nanoparticles. Pure and doped ZnO nanostructures are characterised by using XRD, TEM, FTIR, UV visible spectroscopy and source meter. XRD characterization of pure and doped ZnO nanoparticles were carried out using XPERT Pro X ray Diffractometer with Cu-K$_\alpha$ ($\lambda = 1.544$ Å) radiation between $20°$ and $80°$ of 2θ value. Morphology of nanostructure was studied using TEM, the sample was sonicated for 3 h before TEM investigations in order to stop agglomeration. FTIR and UV visible spectra were studied to find out the characteristic peaks and energy band gap respectively. By using pure and doped ZnO nanostructures for dye sensitised solar cells natural flower made dye was used. I–V characteristic of dye sensitised solar cells were done using Keithley source meter (Model No. 2400) as the voltage source. The set-up used is a two-terminal device in which the nanostructures in a paste form are made using acetic acid are put in the grove made by using a thermoplastic on the surface of the indium tin oxide (ITO). The another ITO is put on the top of the nanostructures. Thermoplastic outside the region of nanofilm also helps to avoid any short circuit between the two electrodes.

3 Results and discussion

3.1 Structural characterization

Figure 1 shows the TEM photographs of the ZnO and Ni doped ZnO showing the flake like shape of the nanostructures. The crystal structures and phase purity of ZnO and Ni doped ZnO nanoparticles were characterised using X-ray diffraction. Figure 2 shows typical spectra of pure ZnO and Zn$_{1-x}$Ni$_x$O (x = 0.00, 0.02, 0.02, 0.06) nanoparticles with well-defined peaks indexed within the hexagonal wurtzite-type structure, in agreement with the standard JCPDS file for ZnO (JCPDS 36-1451). The weak additional peaks corresponding to NiO phase are observed when Ni doping was

increase to 4%. The substitutional limit for doping Ni^{2+} ions into ZnO has also been reported by Anbuselvan et al. [21]. The intensity of NiO peak increases with increasing Ni amount indicating that phase aggregation has occurred and such segregation in the ZnO lattice may be attributed to introduction of a foreign impurity [22].

The crystallite size may be calculated by using Scherrer's formula;

$$D = 0.89\lambda/\beta\,Cos\theta$$

where λ is the wavelength of the incident X-ray, β is the full width at half maxima (FWHM) of the diffraction peak and 2θ is the diffraction angle.

Due to high tendency of agglomeration of nanoparticles it is very hard to determine the particle's size more precisely using TEM observations. The average crystallite size estimated from XRD well matches with the TEM observation.

3.2 Compositional analysis

The chemical bonding in undoped and doped ZnO structure can be analysed using FTIR spectroscopy as shown in Fig. 3. FTIR spectra were recorded in the range of 4000–400 cm^{-1} for all samples. The broad absorption band around 3441 cm^{-1} and the peak at 1605 cm^{-1} is observed corresponding to O–H stretching and bending vibrations of water molecules respectively as the absorption of H$_2$O from moisture and CO$_2$ from the atmosphere could not be avoided. The band at 2349 cm^{-1} was due to O=C=O stretching vibrations which confirms the existence of CO$_2$ while the band at 2931 cm^{-1} was due to C–H stretching vibrations. The band around 1373 cm^{-1} confirms the presence of NO$_3^-$. It is noticed that the doping species affects the spectra and it has been observed that the broadening at the shoulder of ZnO band at 480 cm^{-1} attached to the ZnO peaks which assigned as Ni–O stretching mode. The existence of shift in the frequencies with the increase of dopant concentration (Ni ions) may be due to the difference in the bond length with the replacement of Zn^{2+} with Ni^{2+}, which once again confirms the incorporation of Ni^{2+} into the ZnO lattice [23].

3.3 UV–Visible spectroscopy analysis

Figure 4 shows the absorption spectra of undoped and Ni-doped ZnO nanostructures. The absorption band edge of undoped ZnO is observed at 373 nm and the absorbance increases with the increase in the dopant concentration (Ni^{2+} ions). A shift in absorption band towards longer wavelength region is observed with the addition of 2% Ni^{2+} as well as with the increase in Ni^{2+} concentration from 2 to 4% however the absorption band shifts to lower wavelength when increased from 4 to 6%. The optical band gap was calculated using Tauc's relation as shown in Fig. 5. It is observed
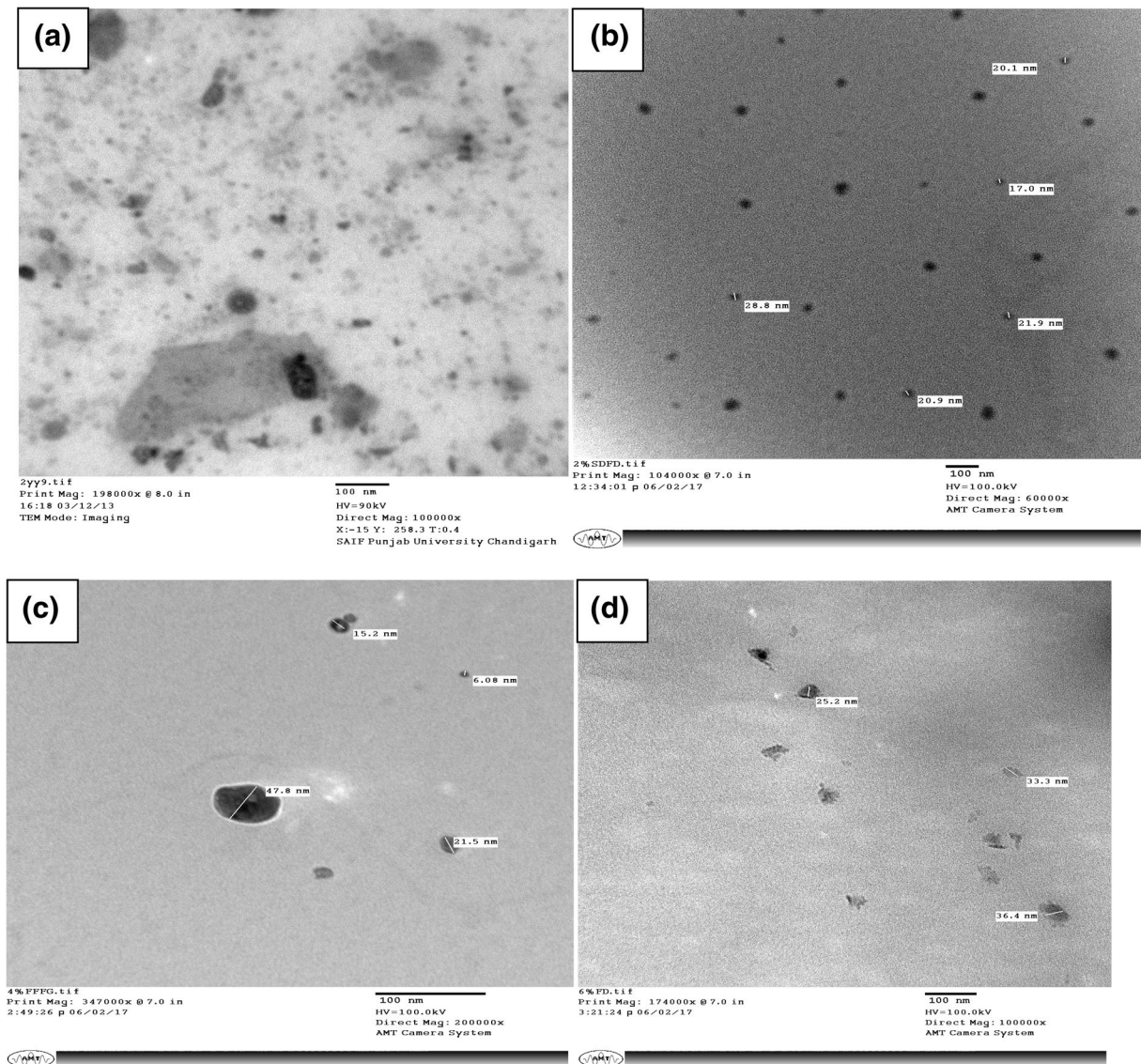
Fig. 1 TEM photographs of **a** undoped ZnO **b** 2% **c** 4% **d** 6% Ni-doped ZnO

that the band gap decreases from 3.80 (undoped ZnO) to 3.54 eV with the addition of 2% Ni^{2+} and further decreased to 3.08 eV with increase in Ni^{2+} dopant concentration from 2 to 4%. This shrinkage of band gap is due to the strain in the crystal lattice [24] and indicates that Ni^{2+} substitute Zn^{2+} within ZnO lattice. As the dopant concentration is further increased to 6%, the band gap increases from 3.80 to 3.96 eV, which may be due to the sp–d interactions taking place between the band electrons and the localised d electrons of Ni^{2+} ions. As the doping is increased to 6%, a shift of Fermi level close to the conduction band (all states close to the conduction are populated) occurs due to Burstein-moss effect which leads to the increase in band gap. Therefore the band gap of ZnO nanostructures can be tuned by varying Ni^{2+} dopant concentration [25]. The humps in the

bandgap graphs are neglected because of the presence of small humps in the actual absorption curve.

3.4 Electrical properties

Figure 6 shows the current–voltage characteristics of undoped and Ni-doped ZnO. It was observed that the current increases with the increase in dopant concentration up to 4% and decreases with the further increase in Ni^{2+} dopant concentration (6%). In the case of 6% Ni-doped ZnO, an electron from the top of the valence band can only be excited into conduction band above the Fermi level (which now lies in conduction band) since all the states below the Fermi level are occupied states, Pauli's exclusion principle forbids excitation into these occupied states which results in decrease
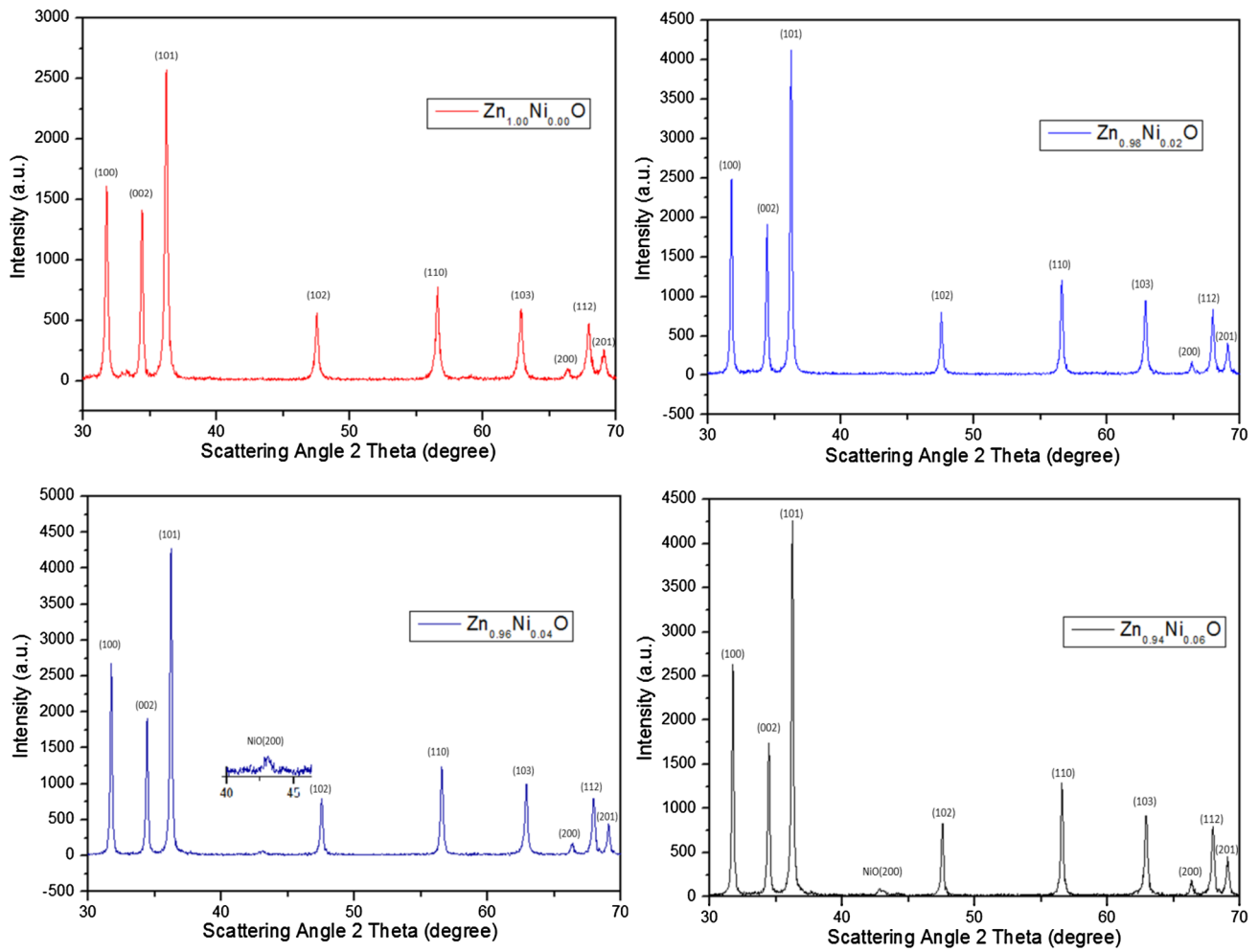
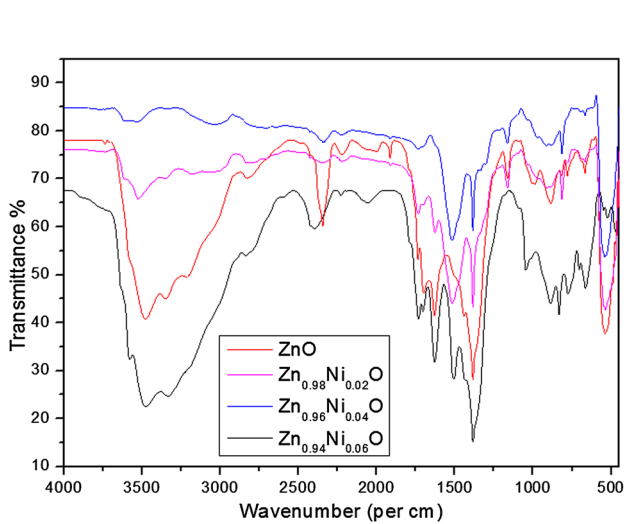**Fig. 2** XRD spectra of undoped and Ni-doped ZnO

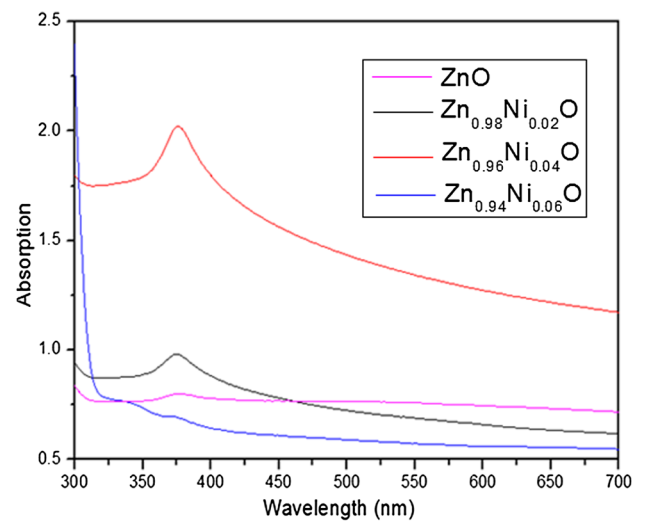**Fig. 3** FTIR spectra of undoped and Ni-doped ZnO

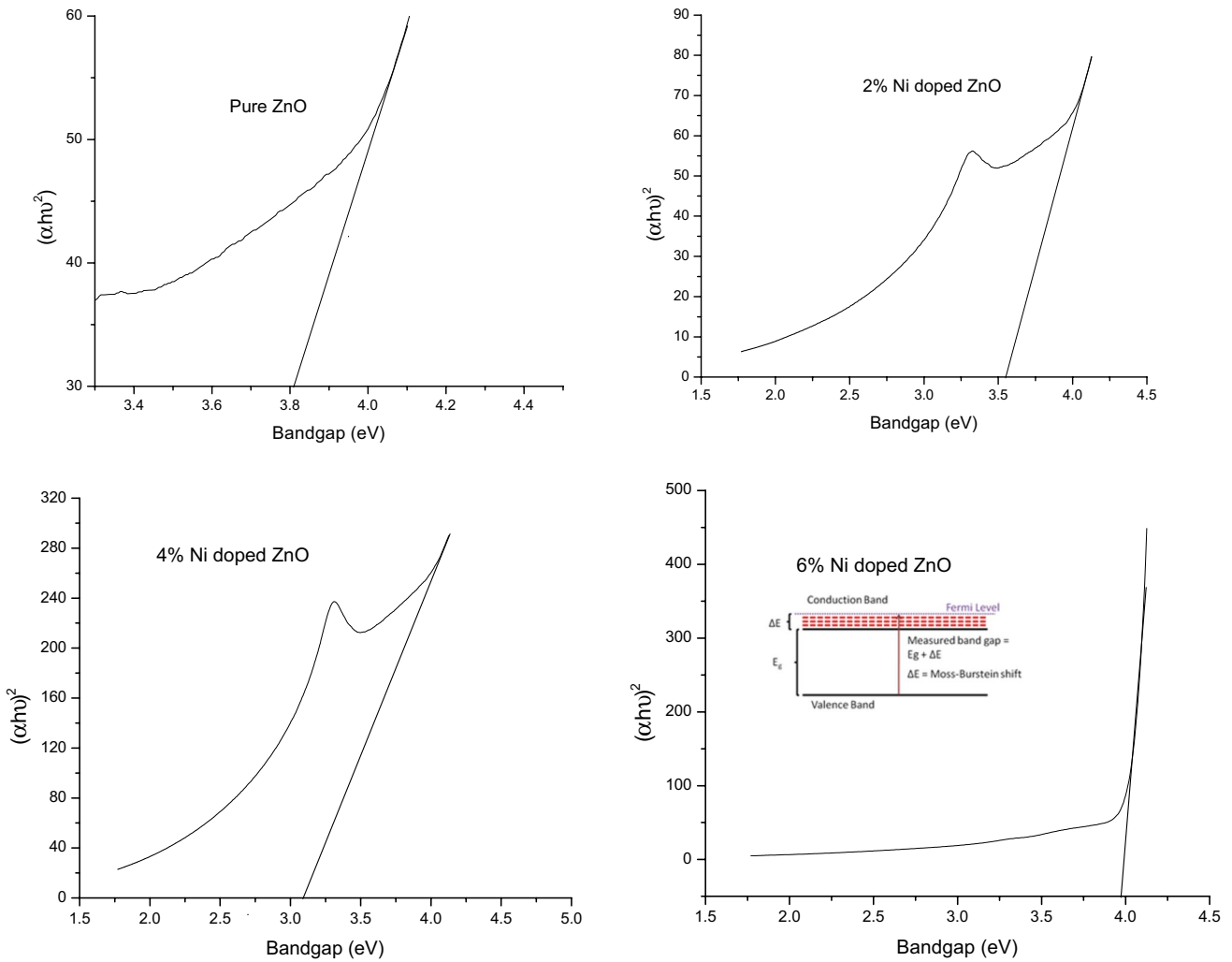**Fig. 4** Absorption spectra of undoped and Ni-doped ZnO

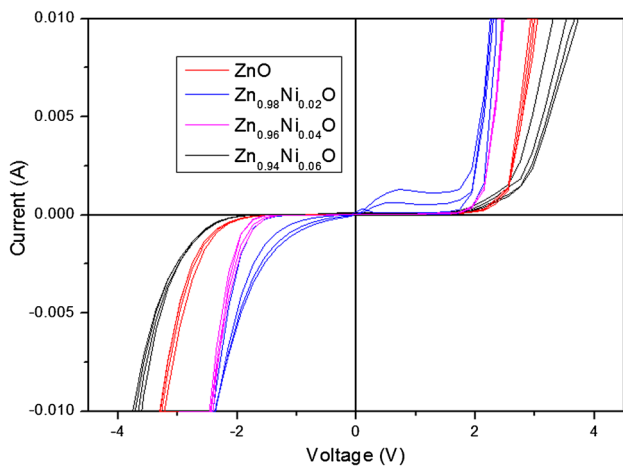**Fig. 5** Energy band gap of undoped and Ni-doped ZnO

Fig. 6 Current–voltage characteristics of undoped and Ni-doped ZnO

of current in 6% Ni doped ZnO. The characteristics were also repeated so as to observe reproducibility of the results as shown in Fig. 6.

4 Conclusions

Nanoparticles of $Zn_{1-x}Ni_xO$ (x = 0.00, 0.02, 0.04, 0.06) have been successfully synthesised by using solution combustion technique. The XRD observations reveal the hexagonal wurtzite structure of undoped and Ni-doped ZnO and the presence of NiO as a secondary phase for 4 and 6% Ni^{2+} doping level. A decrease in energy band gap is observed for doping of Ni^{2+} for 2 and 4% level which may be due to substitution of Ni^{2+} in place of Zn^{2+} in ZnO; whereas increase in energy band gap is observed due to Burstein-Moss effect for 6% Ni^{2+} dopant concentration. The broadening of FTIR spectrum at 480 cm^{-1} also confirms the doping of Ni

(secondary phase of NiO) in ZnO. A decrease of current for higher dopant concentration of Ni (6%) in ZnO is in agreement with the Burstein-moss effect which needs to develop good understanding of the material response to impurities introduced for future practical applications.

References

1. J. Jie, W. Zhang, I. Bello, C.S. Lee, S.T. Lee, One-dimensional II–VI nanostructures: synthesis, properties and optoelectronic applications. Nano Today **5**(4), 313–336 (2010)

2. K.D. Mynbaev, A.V. Shilyaev, A.A. Semakova, E.V. Bykhanova, N.L. Bazhenov, Luminescence of II–VI and III–V nanostructures. Opto-Electron. Rev. **25**(3), 209–214 (2017)

3. A. Mycielski, L. Kowalczyk, R.R. Gałazka, R. Sobolewski, D. Wang, A. Burger, M. Sowinska, M. Groza, P. Siffert, A. Szadkowski, B. Witkowska, W. Kaliszek, Applications of II–VI semimagnetic semiconductors. J. Alloys Compd. **423**, 163–168 (2006)

4. J. Cibert, L. Besombes, D. Ferrand, H. Mariette, Quantum structures of II–VI diluted magnetic semiconductors. Semicond. Semimet. **82**, 287–324 (2008)

5. Z.L.S. Seow, A.S.W. Wong, V. Thavasi, R. Jose, S. Ramakrishna, G.W. Ho, Controlled synthesis and application of ZnO nanoparticles, nanorods and nanospheres in dye-sensitized solar cells. Nanotechnology **20**, 045604 (2009)

6. C. Wang, R. Bao, K. Zhao, T. Zhang, L. Dong, C. Pan, Enhanced emission intensity of vertical aligned flexible ZnO nanowire/p-polymer hybridized LED array by piezo-phototronic effect. Nano Energy **14**, 364–371 (2015)

7. G. Lu, X. Wang, J. Liu, S. Qiu, C. He, B. Li, W. Liu, One-pot synthesis and gas sensing properties of ZnO mesoporous architectures. Sens. Actuators B **184**, 85–92 (2013)

8. Ü. Özgür, V. Avrutin, H. Morkoç, Zinc oxide materials and devices grown by MBE. Molecular Beam Epitaxy, 369–416 (2013)

9. A. Khalid, R. Khan, M. Ul-Islam, T. Khan, F. Wahid, Bacterial cellulose-zinc oxide nanocomposites as a novel dressing system for burn wounds. Carbohydr. Polym. **164**, 214–221 (2017)

10. S. Sharma, V.S. Dalal, V. Mahajan, Synthesis of zinc oxide nano flower for photovoltaic applications. Mater. Today **3**(6), 1359–1362, (2016)

11. A. Zawadzka, P. Płóciennik, J. Strzelecki, B. Sahraoui, Transparent amorphous zinc oxide thin films for NLO applications. Opt. Mater. **37**, 327–337 (2014)

12. W. Yu, L.H. Yang, X.Y. Teng, J.C. Zhang, Z.C. Zhang, G.S. Fu, Influence of structure characteristics on room temperature ferromagnetism of Ni-doped ZnO thin films. J. Appl. Phys. **103**, 093901 (2008)

13. S. Fabbiyola, V. Sailaja, L.J. Kennedy, M. Bououdina, J.J. Vijaya, Optical and magnetic properties of Ni-doped ZnO nanoparticles. J. Alloys Compd., **694**, 522–531 (2017)

14. X. Yan, D. Hu, H. Li, L. Li, X. Chong, Y. Wang, Nanostructure and optical properties of M doped ZnO (M = Ni, Mn) thin films prepared by sol–gel process. Physica B **406**, 3956–3962 (2011)

15. M.S. Abdel-Wahab, A. Jilani, I.S. Yahia, A.A. Al-Ghamdi, Enhanced the photocatalytic activity of Ni-doped ZnO thin films: Morphological, optical and XPS analysis. Superlattices Microstruct. **94**, 108–118 (2016)

16. M.E. Ghazi, M. Izadifard, F.E. Ghodsi, M. Yuonesi, Studying Mn- and Ni-doped ZnO thin films synthesized by the sol-gel method. J. Supercond. Nov. Magn. **25**, 101–108 (2012)

17. A. Yildiz, B. Kayhan, B. Yurduguzel, A.P. Rambu, F. Iacomi, S. Simon, Ni doping effect on electrical conductivity of ZnO nanocrystalline thin films. J. Mater. Sci. **22**, 1473–1478 (2011)

18. X. Wang, L. Zhu, L. Zhang, J. Jiang, Z. Yang, Z. Ye, B. He, Properties of Ni doped and Ni-Ga co-doped ZnO thin films prepared by pulsed laser deposition. J. Alloys Compd. **509**, 3282–3285 (2011)

19. A. Jilani, M.S. Abdel-Wahab, A.A. Al-ghamdi, A. Sadik Dahlan, I.S. Yahia, Nonlinear optical parameters of nanocrystalline AZO thin film measured at different substrate temperatures. Physica B **481**, 97–103 (2015)

20. H.-S. Woo, C.-H. Kwak, J.-H. Chung, J.-H. Lee, Highly selective and sensitive xylene sensors using Ni-doped branched ZnO nanowire networks. Sens. Actuators B **216**, 358–366 (2015)

21. D. Anbuselvan, S. Muthukumaran, Defect related microstructure, optical and photoluminescence behaviour of Ni, Cu co-doped ZnO nanoparticles by co-precipitation method. Opt. Mater. **42**, 124–131 (2015)

22. S. Fabbiyola, L.J. Kennedy, U. Aruldoss, M. Bououdina, A.A. Dakhel, J. Judith Vijaya, Synthesis of Co-doped ZnO nanoparticles via co-precipitation: structural, optical and magnetic properties. Powder Technol. **286**, 757–765 (2015)

23. K.P. Shinde, R.C. Pawar, B.B. Sinha, H.S. Kim, S.S. Oh, K.C. Chung, Optical and magnetic properties of Ni doped ZnO planetary ball milled nanopowder synthesized by co-precipitation. Ceram. Int. **40**, 16799–16804 (2014)

24. K. Karthika, K. Ravichandran, Tuning the microstructural and magnetic properties of ZnO nanopowders through the simultaneous doping of Mn and Ni for biomedical applications. J. Mater. Sci. Technol. **31**, 1111–1117 (2015)

25. S.A. Ahmed, Structural, optical, and magnetic properties of Mn-doped ZnO samples. Results Phys. **7**, 604–610 (2017)